Compressibility Effects

Preliminary calculations of the vorticity Reynolds number profile for a compressible laminar boundary layer shows that the maximum value of this function moves toward the edge of the boundary layer with increasing Mach number and also indicates a decrease in transition Reynolds number with increasing Mach number. Further calculations including heat transfer indicate that at constant Mach number the transition Reynolds number should increase with decreasing wall temperature. These trends are consistent with experiment.

References

[1] van Driest, E. R., "On the aerodynamic heating of blunt bodies," Z. Angew. Math. Phys. **IXb**, 223–248 (March 1958).

[2] Klebanoff, P. S. and Tidstrom, K. D., "Evolution of amplified waves leading to transition in a boundary layer with zero pressure gradient," NASA TN D-195 (September 1959).

[3] Kovasznay, L. S. G., Komoda, H., and Vasudeva, B. R., "Detailed flow field in transition," *Proceedings of the 1962 Heat Transfer and Fluid Mechanics Institute* (Stanford University Press, Stanford, Calif., 1962), pp. 1–26.

[4] Taylor, G. I., "Statistical theory of turbulence, Part V," Proc. Roy. Soc. (London) **A156**, 307–317 (1936).

[5] Dryden, H. L., "Air flow in the boundary layer near a plate," NACA Rept. 562 (1936).

[6] Hall, A. A. and Hislop, G. S., "Experiments on the transition of the laminar boundary layer on a flat plate," Brit. Aeronaut. Res. Comm., Repts. and Memo. 1843 (1938).

[7] Schubauer, G. B. and Skramstad, H. K., "Laminar-boundary-layer oscillations and transition on a flat plate," NACA Rept. 909 (1948).

[8] Falkner, V. M. and Skan, S. W., "Some approximate solutions of the boundary layer equations," Brit. Aeronaut. Res. Comm., Repts. and Memo. 1314 (1939).

[9] Hartree, D. R., "On an equation occurring in Falkner and Skan's approximate treatment of the equations of the boundary layer," Proc. Cambridge Phil. Soc. **33**, 223–239 (1937).

[10] Frössling, N., "Verdunstung, Wärmeübertragung und Geschwindigkeitsverteilung bei zweidimensionaler und rotationssymmetrischer laminarer Grenzschichtströmung," Lunds Univ. Arsskr. Avd. 2 **35**, no. 4 (1940).

[11] Groth, E. E., "Boundary layer transition on bodies of revolution," Northrop Aircraft Rept. NAI-57-1162 (BLC-100) (July 1957).

[12] Schlichting, H., *Boundary Layer Theory* (Pergamon Press, New York, 1955), pp. 218–219.

[13] Boltz, F. W., Kenyon, G. C., and Allen, C. Q., "The boundary-layer transition characteristics of two bodies of revolution, a flat plate, and an unswept wind in a low-turbulence wind tunnel," NASA TN D-309 (April 1960).

[14] Rouse, H., *Elementary Mechanics of Fluids* (John Wiley and Sons Inc., New York, 1946), p. 172.

JUNE 1963 AIAA JOURNAL VOL. 1, NO. 6

Some Characteristics of the Turbulent Boundary Layer with Air Injection

O. E. Tewfik*
University of Minnesota, Minneapolis, Minn.

Measurements of turbulent velocity profiles on a 2-in.-o.d. circular cylinder, aligned with its axis parallel to an approximately 110-fps air stream and with air injection into the boundary layer, are described. The injection rate per unit area of cylinder surface was uniform and equal to 0.00107, 0.00202, 0.00312 of the freestream mass velocity. By means of appropriate mass and momentum balances, the local and average skin friction and the distributions of the radial velocity component and shear through the boundary layer were determined. Study of the results yielded the following. 1) Contrary to the assumption in some theoretical analyses, the radial velocity component was not constant through the boundary layer but increased from its wall value to up to three times as much at the edge of the boundary layer. 2) The assumption that the excess of shear stress in the boundary layer over the wall-shear stress is equal to the product of the mass injection rate per unit area and the local axial velocity component agreed well with the results of measurements in the inner tenth of the boundary layer but became progressively poorer towards the edge of the boundary layer. 3) The local skin friction was found to agree with the measurements of Tendeland and Okuno but to be substantially higher than those of Mickley and Davis and of Pappas and Okuno. 4) The measured ratio of skin friction to its value with no injection agreed well with Rubesin's and Van Driest's analyses for a smooth flat plate but disagreed markedly with Turcotte's analysis. 5) Injection increased all boundary layer thicknesses and distorted the velocity profile from its typically turbulent shape for no injection, the extent of the distortion depending upon the injection rate.

Nomenclature

C_f = dimensionless shear stress $= 2\tau/\rho u_\infty^2$
C_{fw} = local skin friction $= 2\tau_w/\rho u_\infty^2$
C_{fw0} = local skin friction without injection
$\bar{C}_{fw}$ = average skin friction, Eq. (5)
$\bar{C}_{fw0}$ = average skin friction without injection
m = index in power law for boundary layer growth, Eq. (9)
$\dot{m}$ = air mass injection rate per unit area of outer cylinder surface
n = index in power law for velocity u in terms of y, Eq. (9)
p = pressure
q = index in power law for average skin friction in terms of Reynolds number

Received by IAS July 30, 1962; revision received March 21, 1963. Communication from the Heat Transfer Laboratory, Department of Mechanical Engineering, University of Minnesota. The author is grateful to E. R. G. Eckert, Director of the Heat Transfer Laboratory, for valuable discussions, and to L. S. Jurewicz, currently Assistant Research Officer, National Research Council, Ottawa, Canada, for measuring all velocity profiles. This research was supported by the U. S. Air Force through the Air Force Office of Scientific Research of the Air Research and Development Command under Contract AF 49 (638)-558.

* Currently Project Engineer, Corning Glass Works, Corning, N. Y. Member AIAA.

R = cylinder radius
Re_x = Reynolds number $= xu_\infty/\nu$
r = radial distance from cylinder axis
u = axial velocity component
v = radial velocity component
x = axial distance from effective starting point of fully developed turbulent boundary layer
$\bar{x}$ = axial distance from starting of porous section for rough cylinder, or the junction with nosepiece for smooth cylinder
y = radial distance from outer cylinder surface $= r - R$
ν = kinematic viscosity
ρ = density
δ = boundary layer thickness at which $u/u_\infty = 0.99$
δ^* = boundary layer displacement thickness, defined by

$$\delta^*(1 + \delta^*/2R) = \int_0^\infty (1 - u/u_\infty)(r/R)\,dy$$

δ^{**} = boundary layer pseudo-displacement thickness, Eq. (4)
θ = boundary layer momentum thickness, Eq. (3)
η = dimensionless distance from cylinder wall $= y/\delta$
ξ = dimensionless boundary layer thickness $= \delta/R$
τ = shear stress

Subscripts

1 = inside the boundary layer
a = interface between laminar sublayer and turbulent layer
w = at the wall
0 = no injection
∞ = freestream

I. Introduction

THE problem of injection of a fluid through a porous wall into the adjoining boundary layer, thereby modifying the latter's characteristics, is of current interest. Focusing attention on the particular case of flow with slight streamwise pressure gradient and air injection into an adiabatic turbulent boundary layer, a fairly large number of experimental as well as theoretical investigations now are available. Most of the former investigations, however, report the effects of injection on some overall characteristic of the boundary layer such as skin friction. Besides, the range of Reynolds number in some of them is rather limited. Although skin friction in itself is of considerable engineering interest, it is necessary to investigate the details of the flow in the boundary layer for a thorough understanding of the effects of injection. These details include the distributions of the various velocity components and the shear throughout the boundary layer and the growth of the boundary layer. One objective of this paper is to measure and discuss these particular characteristics of the boundary layer in a fairly wide range of Reynolds number.

In theoretical investigations of the effects of injection, several assumptions have been introduced in order to obtain a solution of the governing equations, as is usual in turbulent flow. The validity of each of these assumptions never has been established by measurements. Another objective of this paper is to examine critically some of the assumptions in the light of the results of measurements undertaken.

II. Method of Present Investigation

Consider a circular cylinder with its axis parallel to the direction of motion of an oncoming fluid having a uniform velocity distribution far away from the cylinder, as shown in Fig. 1. This flow model is postulated, since the measurements reported in this investigation were made on a circular cylinder in axial flow. Fluid having the same properties as the main stream is injected at a uniform and steady mass rate per unit area ($\dot{m}$) through the porous walls of the cylinder into the adjacent boundary layer. The radial velocity component at the wall is given by

$$\dot{m} = \rho_w v_w \tag{1}$$

Procedures are presented below to determine some characteristics of the boundary layer, such as local and average skin friction and the distributions of the radial velocity component and the shear throughout the boundary layer, from mass and momentum balances on appropriate control surfaces. To carry out these balances, the distribution of the axial velocity component through the boundary layer, at various axial locations, has to be measured.

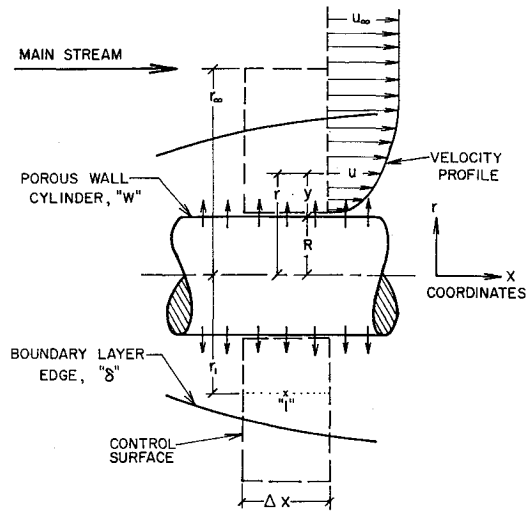

Fig. 1 Flow model and boundary layer

A. Local and Average Skin Friction

A control surface is shown in Fig. 1 in the form of a cylindrical annulus of axial length (Δx) with its plane circular faces cutting through the boundary layer, its outer cylindrical surface in the uniform freestream, and its inner cylindrical surface coinciding with the outer surface of the porous wall of the model. A small pressure gradient in the axial direction of magnitude (dp/dx) exists in the freestream. By Bernoulli's theorem, an axial freestream velocity gradient also exists there and is given by

$$dp/dx = -\rho u_\infty (du_\infty/dx)$$

Mass and momentum balances on the control surface yield the following expression for the local skin friction:

$$C_{fw}/2 = d\theta/dx - v_w/u_\infty - (dp/dx)(2\theta + \delta^{**})/\rho u_\infty^2 \tag{2}$$

where θ is the momentum thickness defined by

$$\theta = \int_0^\infty \left(\frac{u}{u_\infty}\right)\left(1 - \frac{u}{u_\infty}\right)\left(\frac{r}{R}\right)dy \tag{3}$$

and δ^{**} is defined by

$$\delta^{**} = \int_0^\infty \left(1 - \frac{u}{u_\infty}\right)\left(\frac{r}{R}\right)dy \tag{4}$$

In this derivation, the fluid is assumed incompressible.

The average skin friction is defined by

$$\bar{C}_{fw} = \left(\int_0^x C_{fw}\,dx\right)\Big/ x \tag{5}$$

where x is the axial distance measured from the effective starting point of the boundary layer, at which the thickness (momentum or displacement thickness) vanishes. Substitution for C_{fw} from Eq. (2) into Eq. (5) yields

$$\bar{C}_{fw}/2 = \theta/x - v_w/u_\infty - (dp/dx)(2\theta + \delta^{**})/\rho u_\infty^2 \tag{6}$$

with the assumption that the last term does not change with x.

For a turbulent boundary layer, all the dependent variables appearing in Eqs. (2–6) are time-average values; the contribution of the average of products of their fluctuating com-

ponents is assumed negligible. This assumption is justified by the results of measurements of such average products without injection available in the literature.

B. Distribution of the Radial Velocity Component

Let the outer radius of the control surface shown in Fig. 1 shrink from r_∞ to r_1, so that its outside cylindrical surface lies wholly in the boundary layer. A mass balance yields the following expression for the radial velocity component v_1:

$$\left(\frac{r_1}{R}\right)\left(\frac{v_1}{u_\infty}\right) = \left(\frac{v_w}{u_\infty}\right) - d\left[\int_0^{y_1}\left(\frac{u}{u_\infty}\right)\left(\frac{r}{R}\right)dy\right]\Big/dx - \left(\frac{du_\infty}{dx}\right)\left[\int_0^{y_1}\left(\frac{u}{u_\infty}\right)\left(\frac{r}{R}\right)dy\right]\Big/u_\infty \quad (7)$$

Introducing the substitutions

$$\eta = y/\delta \qquad \xi = \delta/R \quad (8)$$

with the assumptions that

$$\xi = A(x/R)^m \qquad u/u_\infty = B\eta^n \quad (9)$$

in which A, B, m, n are constants, into Eq. (7) yields

$$(1 + \eta_1\xi)(v_1/u_\infty) = (v_w/u_\infty) + \eta_1(u_1/u_\infty)[(nm\xi R/x) + \delta(dp/dx)/\rho u_\infty{}^2][1/(n+1) + \xi\eta_1/(n+2)] \quad (10)$$

From Eq. (10), (v_1/u_∞) is a function of the dimensionless distance from the wall η and also of ξ, the ratio of boundary layer thickness to cylinder radius.

C. Distribution of Shear

A momentum balance on the control surface shown in Fig. 1 after shrinking its outer radius from r_∞ to r_1 yields the following equation for C_{f1}, the dimensionless local shear:

$$\left(\frac{C_{f1}}{2}\right)\left(\frac{r_1}{R}\right) - \frac{C_{fw}}{2} = \left(\frac{dp}{dx}\right)\left[\int_0^{y_1}\left(\frac{r}{R}\right)dy\right]\Big/\rho u_\infty{}^2 + d\left[\int_0^{y_1}\left(\frac{u}{u_\infty}\right)^2\left(\frac{r}{R}\right)dy\right]\Big/dx + \left(\frac{r_1}{R}\right)\left(\frac{u_1}{u_\infty}\right)\left(\frac{v_1}{u_\infty}\right) + \left(\frac{2}{u_\infty}\right)\left(\frac{du_\infty}{dx}\right)\int_0^{y_1}\left(\frac{u}{u_\infty}\right)^2\left(\frac{r}{R}\right)dy \quad (11)$$

Introducing the substitutions given by Eq. (8) and the assumptions given by Eq. (9) into Eq. (11) yields the following expression for C_{f1}:

$$(1 + \eta_1\xi)\left(\frac{C_{f1}}{2}\right) = \left(\frac{C_{fw}}{2}\right) + \left(\frac{v_w}{u_\infty}\right)\left(\frac{u_1}{u_\infty}\right) - \eta_1\left(\frac{u_1}{u_\infty}\right)^2\left(\frac{nm\xi R}{x} + \frac{\delta}{\rho u_\infty{}^2}\frac{dp}{dx}\right)\left(\frac{1}{2n+1} + \frac{\eta_1\xi}{n+2}\right)\Big/(n+1) + \delta\eta_1\left[1 + \left(\frac{\eta_1\xi}{2}\right)\right]\left(\frac{dp}{dx}\right)\Big/\rho u_\infty{}^2 \quad (12)$$

Notice that C_{f1} and v_1 depend on ξ and η. Similar mass and momentum balances for a flat plate will yield C_{f1} and v_1 as function of η only, and hence the appearance of the parameter ξ must be due to the cylindrical geometry. Inspection of Eqs. (2, 10, and 12) shows that it is only necessary to measure velocity profiles at several axial locations in order to determine C_{fw} and the distributions of v/u_∞ and C_f.

III. Apparatus and Experimental Procedure

The model, shown in Fig. 2, is a 2-in.-o.d. circular cylinder having an ogival nosepiece followed by a porous section and an afterbody. The outer shell of the porous section was rolled out of a thin screen woven from stainless steel wire.

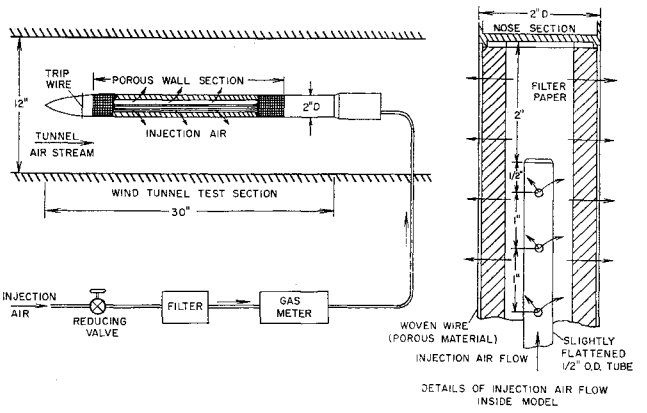

Fig. 2 Schematic of injection air flow system

The weaving, sintering, and calendering processes done to the screen resulted in the formation of small depressions in the outside model surface approximately 0.005 in. deep.

The cylinder was aligned with its axis parallel to the air stream in the 1 × 2 ft test section of the closed circuit continuously operating wind tunnel of the Heat Transfer Laboratory. The speed of the air stream was around 110 fps and its turbulence level 0.2%. Air from a compressor facility was ducted to the inside of the model and injected at a prescribed mass rate through the model porous walls into the boundary layer. The distribution of the injection rate over the porous wall was found by measurements to be uniform within ±4%. An American iron case gas meter measured the volume of injected air with an accuracy of ±1%. By means of a timer and by measuring the density of the air at the meter outlet, the air mass injection rate was determined.

At each of three air injection rates, velocity profiles throughout the boundary layer were measured at various axial locations by means of an impact probe made out of flattened hypodermic tubing. The mouth of the probe measured 0.006 × 0.040 in. on the outside, and its wall thickness was 0.001 in. The probe was attached to a micrometer, from the readings of which its distance from the model wall was determined.

IV. Results

There was a slight pressure drop in the tunnel test section, amounting to about 0.1 in. of oil in a distance of 20 in. In order to calibrate the apparatus, velocity profiles first were measured without injection. The average skin friction was

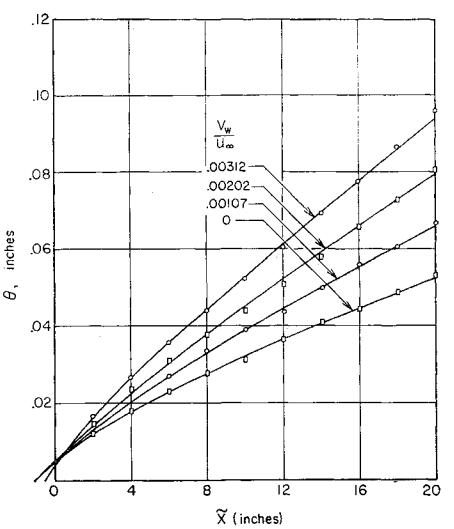

Fig. 3 Effective starting point of boundary layer at various injection rates

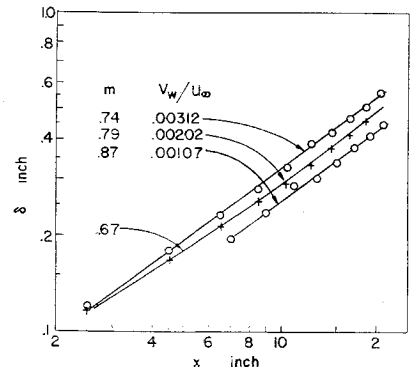

Fig. 4 Effect of injection on boundary layer development

determined from Eq. (6) and the local skin friction from Eq. (2) by numerical differentiation of the momentum thickness. When compared with the Prandtl-Schlichting semi-empirical correlation[7] for a smooth flat plate, they are larger by about 25% in both cases. The discrepancy may be attributed mainly to surface roughness.

In order to investigate more thoroughly the effects of surface roughness, velocity profile measurements were carried out on an almost identical but smooth and nonporous cylindrical model previously constructed for other investigations.[8] The focal and average skin frictions were higher than the Prandtl-Schlichting correlation by about 10%, which is within the scatter of the data of various investigators of skin friction on a smooth flat plate.[7] Hence, the method of measuring skin friction was considered satisfactory.

Next, velocity profiles of the boundary layer were measured at various axial locations at each of three injection rates given by v_w/u_∞ = 0.00107, 0.00202, 0.00312. The momentum thickness, displacement thickness, and 99% thickness of the boundary layer were determined. Figure 3 presents the growth of the momentum thickness along the model. By extrapolation to zero thickness, the effective starting point of the boundary layer for each injection rate was determined within $\pm\frac{1}{4}$ in. Next, the exponent m, describing the growth of the boundary layer according to the relation $\delta = Cx^m$, was determined by plotting the boundary layer thickness vs the axial distance measured from the effective starting point in logarithmic coordinates, as shown in Fig. 4. It is clear that, at a given x, δ and θ increase with the injection rate. It also is observed that the rate of boundary layer growth slightly decreases as the injection rate increases.

Similarity of the velocity profiles was investigated for the largest injection rate by plotting u/u_∞ vs y/δ^* in Fig. 5 and vs y/δ in Fig. 6. It is apparent that all the points lie close to a single curve, and hence it may be concluded that similarity exists, at least within the range of Reynolds number of the experiments.

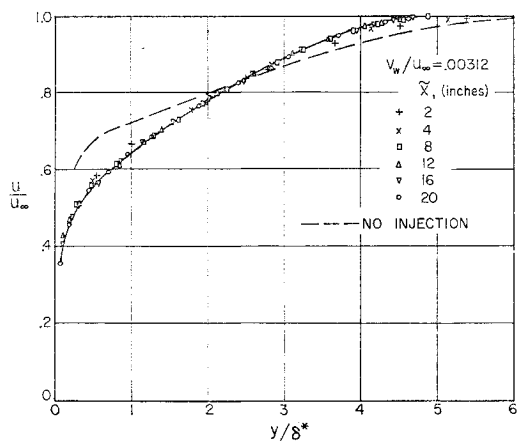

Fig. 5 Effect of injection on velocity profile

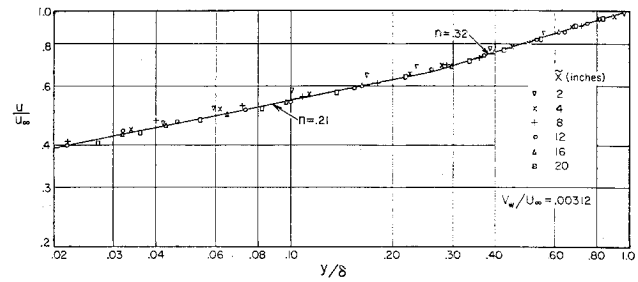

Fig. 6 Similarity of velocity profiles with injection

The profile shape at the highest injection rate is compared in Fig. 5 with that without injection. It is clear that the injection process affects the velocity distribution throughout the entire boundary layer. A similar conclusion was made in studying velocity profiles on a flat plate with air injection.[9] The profiles for the smaller values of the injection rate exhibit the same trend but with progressively smaller deviations from the zero injection profile as the injection rate is decreased.

From Fig. 6, it appears that the velocity distribution does not obey the same power law throughout the entire thickness of the boundary layer. Near the wall, the index n is 0.21, whereas in the outer three quarters of the boundary layer it is 0.32.

A. Skin Friction

Local and average skin friction were calculated from Eqs. (2) and (6), and the results are presented in Figs. 7a–7c as a function of Reynolds number, with the injection rate as parameter. The characteristic length in the Reynolds number is the axial distance from the effective starting point of the boundary layer. The data points for the average skin friction are quite smooth, but those for the local skin friction exhibit a rather large scatter of up to ±15% in some cases. This scatter is due to the procedure for obtaining the local skin friction by numerical differentiation of the measured momentum thickness. In fairing a best fit for such scattered data points, two guiding steps were followed:

1) It is clear from Fig. 7 that on roughly the first half of the model the average skin friction obeys a power law, say,

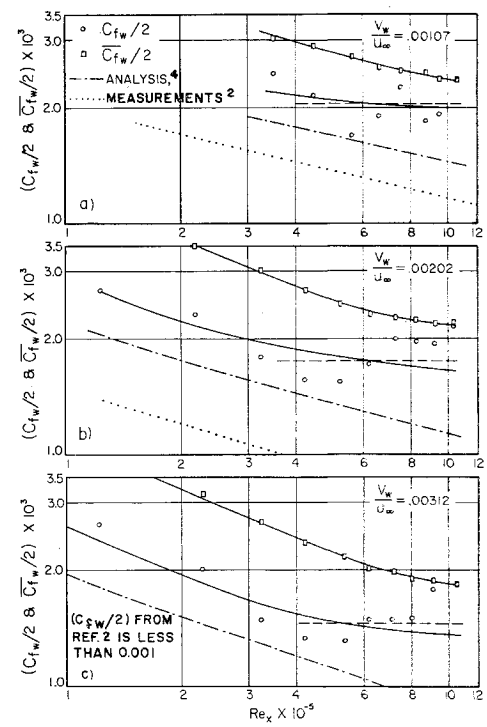

Fig. 7 Effect of injection on local and average skin friction

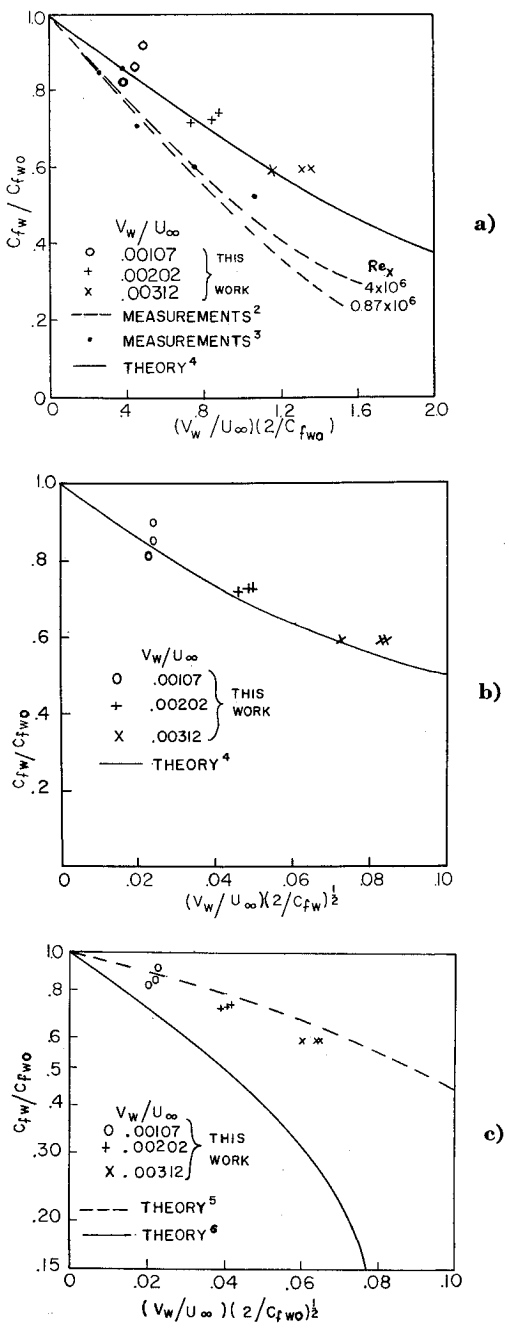

Fig. 8 Reduction of skin friction with injection

$\bar{C}_{fw} \sim Re_x^q$, in which q can be determined fairly accurately from the slope of the graph. Since $C_{fw} = d(\bar{C}_{fw} \cdot x)/dx$, it follows that $C_{fw} = (q + 1)\bar{C}_{fw}$. In this way, C_{fw} was determined along the first half of the model from the well-defined curve for $\bar{C}_{fw}$.

2) On the latter half of the model, the average skin friction was determined by fitting the measured momentum thickness by a straight line and computing the slope of this straight line. It is shown in Fig. 7 as a dashed line. The curve for C_{fw} has to satisfy the condition that this dashed line represents the average of the local C_{fw} values on the latter half of the model. With this stipulation as a guide, the best fit for C_{fw} was determined along the latter half of the model.

1. *Comparison with previous measurements*

The results of the present measurements now will be compared with those of Mickley and Davis.[2] In this latter work, a flat plate fabricated from an 80-mesh screen, 12-ft long by 1-ft wide, was incorporated into the walls of the test section of a low-speed wind tunnel, with boundary layer removal ahead of the plate leading edge. Air was injected at a uniform rate per unit plate area of up to 0.005 of the freestream mass velocity. The Reynolds number was formed with the distance from the leading edge as characteristic length, and its range was extended from about 2×10^5 to 3×10^6. Local skin friction was determined from the rate of growth of the momentum thickness along the plate, obtained from measurements of velocity profiles. Figure 7 shows the present measurements to be higher than those of Mickley and Davis by about 50% at the smallest injection rate, and by up to about 150 to 200% at the highest common injection rate, depending upon Re_x.

Since the experimental conditions were about the same in both cases, such as the roughness of the model surface, the freestream Reynolds number range and its Mach number, and the method of calculating skin friction, it is interesting to investigate the reasons for such appreciable discrepancy. These appear to be the following. First, Mickley and Davis neglected the contribution to skin friction of the pressure gradient term in Eq. (2). On examining their data, the pressure gradient along the plate, although small in absolute value, cannot be neglected in comparison with the small difference between the two other terms in the right-hand side of Eq. (2). When taken into consideration, it would increase their skin friction values by about 15% at the smallest injection rate and 50% at the highest common injection rate. Second, there is a question of accuracy of calibration of the apparatus of Ref. 2, since the surface roughness of the plate failed to show any effect on skin friction for the case of zero injection. This is rather surprising, since the turbulent boundary layer is known to be sensitive to surface roughness.[10] In particular, such roughness in the present measurements was shown to increase the skin friction by about 15%.

The extent of the reduction in skin friction due to injection is compared in Fig. 8a with the results of Pappas and Okuno[3] obtained by direct measurements of drag forces on a smooth 15° porous core, aligned with its axis parallel to a Mach 0.3 air stream. Garnet paper glued to the cone nose piece served as boundary layer trip. The Reynolds number ranged from about 0.9×10^6 to 5.9×10^6, and its characteristic length was the length of ray of the cone measured from its tip. The present measurements are higher by up to about 25%. The discrepancy may be due to some difficulties in directly measuring the drag force and the neglect of pressure gradient along the cone in computing skin friction.

2. *Comparison with theory*

At present, many analyses are available for predicting the effects of air injection. The analyses of Rubesin[4] and of Van Driest[5] are very similar. In either, the boundary layer is divided into a laminar sublayer and a fully turbulent outer layer. The turbulent shear stress was related to the distance from the wall by a Prandtl mixing length hypothesis. The constant in the mixing length and the value of $u_a/(\tau/\rho)^{1/2}$ were assumed identical with their values at zero injection. The two analyses differ in their choice of the injection parameter, namely, $(v_w/u_\infty)\ (2/C_{fw})$ and $(v_w/u_\infty)\ (2/C_{fw})^{1/2}$, respectively. Since a relation between C_{fw} and Re_x with either injection parameter readily can be transformed into another relation in terms of the other injection parameter, either parameter may be chosen for data correlation.

For engineering purposes, the reduction in skin friction is of particular interest. The relation between (C_{fw}/C_{fw0}) and the injection parameter turns out to be a weak function of the axial Reynolds number or freestream Mach number. For convenience in applications, the injection parameter appears to be either $(v_w/u_\infty)\ (2/C_{fw0})$ or $(v_w/u_\infty)\ (2/C_{fw0})^{1/2}$. From Figs. 8a–8c, the present measurements show satisfactory agreement with Rubesin's and Van Driest's analyses.[4, 5] No clear advantage of the choice of any injection parameter could

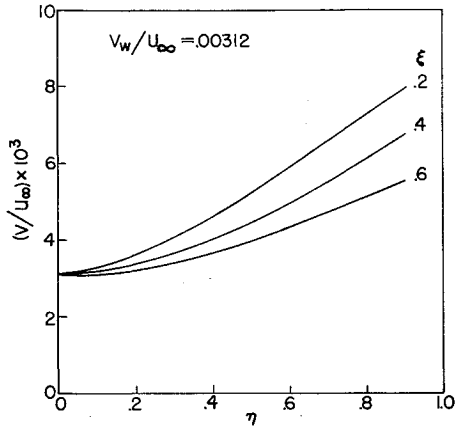

Fig. 9 Distribution of radial velocity with injection

be distinguished, however. Good agreement between Rubesin's analysis and the measurements of Tendeland and Okuno has been reported elsewhere.[1] Hence, the present measurements agree satisfactorily with those of Ref. 1.

The analysis of Turcotte[6] divides the boundary layer into a fully turbulent outer layer and a sublayer in which both laminar and turbulent shear stresses occur right up to the wall. The turbulent shear stress was related to the distance from the wall and the local velocity by a Rannie eddy diffusivity formula. The injection process was assumed to affect only the sublayer. From Fig. 8c, its predictions disagree markedly with the present measurements, although they were shown elsewhere[6] to agree quite well with the measurements of Mickley and Davis. From Fig. 5, it is evident that the injection process affects the velocity distribution in the entire boundary layer. Later, it will be shown that it affects also the shear stress distribution. Hence, a basic assumption in Turcotte's analysis does not agree with the present measurements, which may account for the observed discrepancy.

A question was raised by Leadon[9] regarding which of the injection parameters $(v_w/u_\infty)\ (2/C_{fw0})^{1/2}$ or $(v_w/u_\infty)\ (2/C_{fw0})$ would correlate best the skin friction predictions or measurements. From the present measurements as presented in Figs. 8a–8c, no clear advantage of any particular parameter could be distinguished.

From the foregoing comparison of the results of the present measurements with pertinent theory, it would appear that the Prandtl mixing length hypothesis for the turbulent shear stress offers at present the best means of predicting the effects of injection on skin friction with reasonable accuracy.

B. Distribution of the Radial Velocity Component

This is presented in Fig. 9 for the highest injection rate. For smaller injection rates, the distributions are similar, and at a given ξ they increase progressively from zero injection to maximum injection. It is seen that the radial velocity component increases steadily from its wall value to almost two to three times as much at the edge of boundary layer. In many analytical studies of injection,[4, 5] the radial velocity component is considered constant throughout the boundary layer. This assumption is therefore not strictly valid, except perhaps in the inner quarter of the boundary layer, and even then it is a rough approximation. Also, its deviation from the results of measurements becomes progressively more pronounced as the injection rate is increased.

C. Distribution of Shear

This is presented in Figs. 10a and 10b for the highest injection rate. Similar curves were obtained for the other injection rates. For one particular value of ξ of 0.4, the distribution is shown in Figs. 11a and 11b for all injection rates.

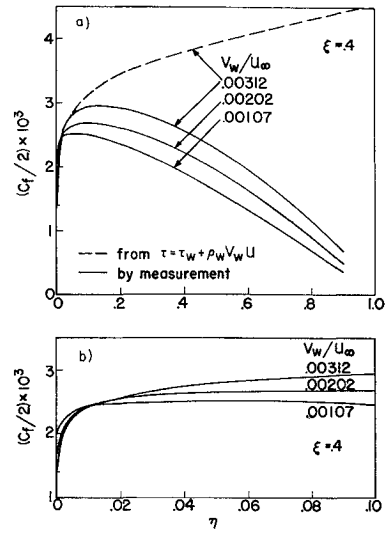

Fig. 10 Distribution of shear at a given injection rate

For the sake of clarity, the distributions close to the wall, in the inner tenth of the boundary layer, are shown separately. From these figures, it is clear that, with increasing injection, the shear stress at the same value of η and ξ decreases at the wall and in its immediate vicinity but increases in the remainder of the boundary layer. Hence, the injection process affects the shear stress throughout the entire boundary layer and not just in the sublayer region as assumed in the analysis of Turcotte.[6]

In many analyses,[4, 5] the following assumption is made regarding the shear stress in the boundary layer:

$$\tau = \tau_w + \rho_w v_w u$$

From this, it follows that

$$C_f/2 = C_{fw}/2 + (v_w/u_\infty)(u/u_\infty) \qquad (13)$$

Equation (13) is plotted in Figs. 10 and 11 as a dashed line and compared with the results of the present measurements. The deviation is less than 5% in approximately the inner tenth of the boundary layer, and hence the assumption may be considered satisfactory in the vicinity of the wall. Beyond that, the assumption becomes progressively poorer. Similar conclusions hold when $\xi = 0.6$ and also for the other injection rates.

There is a question as to why the predictions of Refs. 4 and 5 show good agreement of skin friction with the present measurements, in spite of the poor agreement of Eq. (13)

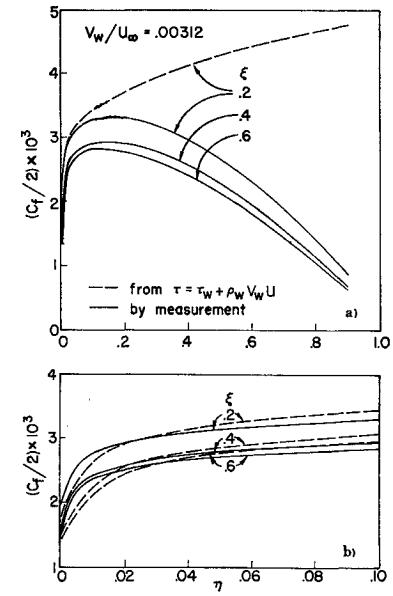

Fig. 11 Effect of injection on distribution of shear

with the same measurements throughout the outer four fifths of the boundary layer. It must be that an overall characteristic of the boundary layer such as skin friction is not sensitive to the detailed shear distribution assumed in Eq. (13). A similar situation exists in the case of zero injection and also in the insensitivity of skin friction to the velocity profile across the boundary layer.

V. Summary and Conclusions

A 2-in.-o.d. circular cylinder with porous woven-wire walls was aligned with its axis parallel to an air stream having a velocity of approximately 110 fps. The boundary layer was turbulent. Velocity profiles at various axial locations were measured by a suitable Pitot tube when air was injected through the cylinder walls into the adjacent boundary layer at a uniform mass rate per unit outer cylinder area equal to 0, 0.00107, 0.00202, and 0.00312 of the freestream mass velocity. From these measurements, the boundary layer momentum thickness, displacement thickness, and 99% thickness were determined, and the effective starting point of the turbulent boundary layer was located for each injection rate. By means of appropriate mass and momentum balances, it was possible to compute the distributions of the local and average skin friction along the model and the distributions of the radial velocity component and the shear throughout the boundary layer.

The results for skin friction are presented as a function of Reynolds number, with the injection rate as parameter. The Reynolds number was formed with the axial distance from the effective starting point as characteristic length, and its range extended from about 10^5 to about 1.1×10^6.

The results for the distribution of the radial velocity component and shear in the boundary layer are presented as a function of the dimensionless distance from the cylinder wall, with the ratio of boundary layer thickness to cylinder radius as parameter. This latter parameter is a consequence of the cylindrical geometry.

The outside surface of the porous walls of the model is not hydraulically smooth. Hence, in order to investigate the effects of surface roughness, similar measurements were taken on a smooth but otherwise identical cylinder, without any injection. On comparing the results for the two cylinders, surface roughness increased the skin friction by about 15% at the same Re_x. For the smooth cylinder, the skin friction is larger by about 10% than the Prandtl-Schlichting correlation for a smooth flat plate.

The results of measurements with air injection indicate the following effects of injection on some characteristics of the turbulent boundary layer:

1) At a given Reynolds number, all the boundary layer thicknesses are increased. Their rate of growth along the model is decreased somewhat.

2) Injection has a pronounced effect on the shape of the velocity profile throughout the entire boundary layer.

3) At a given Reynolds number, the skin friction is reduced by injection. At the highest injection rate, it is about 25% larger than the predictions of Rubesin's analysis for a smooth flat plate.[4] This discrepancy is believed to be due to surface roughness. When the ratio of local skin friction with injection to that without injection is compared with Rubesin's analysis,[4] good agreement is obtained, indicating that in this form of presentation surface roughness effects largely cancel out. Maximum reduction in skin friction due to injection obtained in this work is about 50%.

4) Good agreement also was obtained with Van Driest's analysis[5] and with the measurements of Tendeland and Okuno.[1] The present measurements are higher than the predictions of Turcotte's analysis[6] by up to about 100%. The assumption made in the analysis that the injection process affects the sublayer only may have caused this discrepancy. At a given Reynolds number, the measured skin friction was higher than the measurements of Mickley and Davis,[2] and the discrepancy increases as the injection rate increases, amounting to about 200% at the highest injection rate. An important contribution to this discrepancy is the neglect of the pressure gradient term in computing the skin friction.

5) The radial velocity component increases with injection, and its value at the edge of boundary layer is up to three times its value at the wall. Contrary to assumptions made in various analyses,[4, 5] therefore, it cannot be regarded as constant throughout the boundary layer.

6) At a given value of ξ, injection reduces the friction factor at the wall and in its immediate vicinity approximately in the inner tenth of the boundary layer. Beyond that, the converse happens. The assumption proposed in various analyses[4, 5] regarding the shear stress in the boundary layer, namely, $\tau = \tau_w + \rho_w v_w u$, agrees within 3% with the results of measurements reported here in the inner fifth of the boundary layer. However, it becomes increasingly poor beyond that distance as the edge of the boundary layer is approached.

References

[1] Tendeland, T. and Okuno, A. F., "The effect of fluid injection on the compressible turbulent boundary layer—the effect on skin friction of air injected into the boundary layer of a cone at $M = 2.7$," NACA RM A56 DO 5 (1956).

[2] Mickley, H. S. and Davis, R. S., "Momentum transfer for flow over a flat plate with blowing," NACA TN 4017 (1957).

[3] Pappas, C. C. and Okuno, A. F., "Measurements of skin friction of the compressible turbulent boundary layer on a cone with foreign gas injection," J. Aerospace Sci. **27**, 321–331 (1960).

[4] Rubesin, M. W., "An analytical estimation of the effect of transpiration cooling on the heat-transfer and skin-friction characteristics of a compressible, turbulent boundary layer," NACA TN 3341 (1954).

[5] Van Driest, E. R., "On the aerodynamic heating of blunt bodies," Z. Angew. Math. Phys. **IXb**, 233–248 (1958).

[6] Turcotte, D. L., "A sublayer theory for fluid injection into the incompressible turbulent boundary layer," J. Aerospace Sci. **27**, 675–678 (1960).

[7] Schlichting, H., *Boundary Layer Theory* (McGraw-Hill Book Co. Inc., New York, 1960), 4th ed., pp. 538–540.

[8] Eichorn, R., Eckert, E. R. G., and Anderson, A. D., "An experimental study of the effects of non-uniform wall temperature on heat transfer in laminar and turbulent axisymmetric flow along a cylinder," J. Heat Transfer **82**, 349–359 (1960).

[9] Leadon, B. M., "Comments on 'A sublayer theory for fluid injection,'" J. Aerospace Sci. **28**, 826–827 (1961).

[10] Clauser, F. H., *Advances in Applied Mechanics* (Academic Press Inc., New York, 1956), Vol. 4, pp. 1–51.